Petroleum 3 (2017) 144–154

Contents lists available at ScienceDirect

Petroleum

journal homepage: www.keaipublishing.com/en/journals/petlm

Preliminary assessment of CO_2 injectivity in carbonate storage sites

Arshad Raza [a, *], Raoof Gholami [a], Reza Rezaee [b], Chua Han Bing [c], Ramasamy Nagarajan [d], Mohamed Ali Hamid [a]

[a] Department of Petroleum Engineering, Curtin University, Malaysia
[b] Department of Petroleum Engineering, Curtin University, Australia
[c] Department of Chemical Engineering, Curtin University, Malaysia
[d] Department of Applied Geology, Curtin University, Malaysia

ARTICLE INFO

Article history:
Received 19 May 2016
Received in revised form
19 November 2016
Accepted 21 November 2016

Keywords:
CO_2 storage
Injectivity
Carbonate reservoir
Lithofacies
Petrophysics

ABSTRACT

Depleted gas reservoirs are used for a large-scale carbon dioxide (CO_2) storage and reduction of the greenhouse gas released into the atmosphere. To identify a suitable depleted reservoir, it is essential to do a preliminary and comprehensive assessment of key storage factors such as storage capacity, injectivity, trapping mechanisms, and containment. However, there are a limited number of studies providing a preliminary assessment of CO_2 injectivity potential in depleted gas reservoirs prior to a CO_2 storage operation. The aim of this study is to provide a preliminary assessment of a gas field located in Malaysia for its storage potential based on subsurface characterization prior to injection. Evaluation of the reservoir interval based on the facies, cores, and wireline log data of a well located in the field indicated that the pore type and fabrics analysis is very beneficial to identify suitable locations for a successful storage practice. Although the results obtained are promising, it is recommended to combine this preliminary assessment with the fluid-mineral interactions analysis before making any judgment about reliability of storage sites.

1. Introduction

It is generally known that CO_2 can be safely stored in depleted oil and gas reservoirs through a large-scale injection operation [1–4]. Depleted gas reservoirs are the best candidates for the storage practice due to their proven storing capacity, suitable petrophysical characteristics, and in place infrastructures [5]. Retrograde gas reservoirs, in particular, may have dual applications, on these occasions, and CO_2 injection may help to have a better gas and condensate recovery, due to re-vaporization and reservoir re-pressurization [6,7]. Comparatively, depleted condensate gas reservoirs are more favourable then condensate gas because of their higher compressibility which is the sign of a high storage capacity [8]. However, there are many studies carried out in recent years pointing out the significance potential of a condensate gas reservoir as a suitable storage site [6,7,9–11].

To identify a suitable CO_2 storage medium, a preliminary analysis is performed based on different screening criteria [12–14]. This is followed by the analysis of storage capacity [15,16], injectivity [16–20], trapping mechanisms [16,21–23], and reservoir/seal integrity [5,16,24] through numerical and lab based techniques. A comprehensive injectivity analysis based on facies and petrophysical descriptions is one of the strategies taken as a part of the storage site selection [25,26], where few important indicators are selected to highlight the potential zones for a favourable CO_2 storage.

Upon injection, CO_2 changes its phase and becomes a dense (supercritical) fluid at the pressure and temperature of higher than 30.98 °C (87.76 °F) and 7.38 MPa (1070 psi), respectively. This density can also be achieved at a depth of greater than 2625 ft (800 m), in a low temperature gradient medium where

* Corresponding author.
E-mail address: Arshadraza212@gmail.com (A. Raza).
Peer review under responsibility of Southwest Petroleum University.

Production and Hosting by Elsevier on behalf of KeAi

http://dx.doi.org/10.1016/j.petlm.2016.11.008

the pressure would be a key factor to achieve the supercritical condition [27,28], which favours the injectivity potential [29] because a dense CO_2 occupies smaller pore volumes [19]. Furthermore, porosity, permeability and heterogeneity are major factors controlling an effective CO_2 storage capacity [26,30,31]. Particularly, permeability along with the thickness of the targeted medium are the key parameters for a successful injectivity [29], which ultimately controls the cost and efficiency of the injection operation [32,33]. Residual gas [18,34] and condensate (oil phase) saturations [35] are other factors which are linked to an efficient injectivity. A high percentage of water or gas saturation can also reduce the chance of having an effective storage capacity [34,36,37]. The amount of remaining oil in a retrograde reservoir significantly affects the relative permeability and injectivity of a depleted site [35]. On the other hand, the heterogeneity level of the storage medium controls the brine displacement which has a significant influence on the plume migration and storage capacity [38,39]. These properties have gained a lot of attention during the preliminary assessment of any geologic mediums for a storage practice in the past decade [14,18,19,26–28,31,40–45] as highlighted in Table 1.

There are, however, few mechanisms which may cause complications in the analysis. For instance, if a formation is composed of carbonates, the geochemical reactions between brine and formation rocks increase the pH of brine causing an enhanced CO_2 solubility upon injection [46,47]. Carbonates like calcite, magnesite and siderite are more likely to precipitate as reacting cations because of dissolution reactions with carbonate brine [48] as given in Table 2. These precipitation reactions may occur in a relatively short period of time in carbonates compared to silicate minerals which can be a function of the pressure and temperature variation. Changes induced due to the precipitation depend on mineralogy and permeability of formations and often affect the rock characteristics [29]. For instance, Mohamed and Nasr-El-Din [49], experimentally tested heterogeneous Silurian dolomite and heterogeneous Indiana limestone. Their study indicated that more damages are induced on heterogeneous rocks compared to the homogeneous cores because of high precipitation reactions taking place in high permeability rocks [49]. However, some researches carried out in recent years have shown that even the rock permeability reduction causes a significant drop in injectivity [50–55], although carbonate mineralization [56] and mineral dissolution may also contribute into this decline [54]. This mineral dissolution and precipitation may also have an impact on the storage integrity during and after injection which may lead to damage to the wellbores, the overlying seal, and any fault/seal systems. Therefore, it is essential to evaluate CO_2/brine/rock chemical reactions during and after any storage practices [57,58]. Therefore, carbonates are not easy rocks to characterize due to their complex pore structures, micro-porosities, wide heterogeneities, and high reactivity [57,59].

The aim of this study is to perform a preliminary assessment for injectivity in a carbonate gas field located in Malaysia. Having known that porosity, permeability and thickness favour injectivity, two steps are taken to achieve the objective of this study: 1) characterization of the reservoir in terms of its lithological and petrophysical properties based on the core description, well log, and facies analysis, and 2) discussing the relationship between petrographical and petrophysical properties of the medium with CO_2 injectivity.

2. Site description

The field of this study is one of the major retrograde gas fields in a Miocene age sedimentary basin of Malaysia. The Miocene age geologic succession of the field consists of the transgressive cap phase, intermediate phase, main build-up phase upper, and main build phase lower which are mainly divided into five zones. The reservoir is capped by a massive shale rock (>500 m) and

Table 1
The proposed indicators to justify the good zones for favourable CO_2 storage.

Parameters	Positive indicators	Cautionary indicators	Indication of aspect	Reference
Depth	>800 m	800 m > depth > 2000 m	Storage capacity	[27,28,45]
CO_2 density	high	low	Storage capacity	[19,45]
Porosity	>20%	<10%	Storage capacity	[30,31,45]
Thickness	≫50 m	<20 m	Injectivity	[30,31,45]
Permeability (near-wellbore)	>100mD	10–100mD	Injectivity	[30,31,45]
Pore throat size distribution	less heterogeneous	highly heterogeneous	Injectivity	[45]
Residual gas/water saturation	low	high	Injectivity	[18,34,45]
Condensate (oil phase) saturation	low	high	Injectivity	[35]
Lithofacies types	Good Quality	Low Quality	Injectivity	[26]

Table 2
Mineral-CO_2-brine interactions taking place in reservoirs [48].

Primary mineral	Reaction	Secondary mineral
Dissolution Reactions	$CO_2(g) \rightarrow CO_2(aq)$	
	$CO_2(g) + H_2O(l) \rightleftharpoons H_2CO_3(aq)$	
	$H_2CO_{3(}aq) \rightleftharpoons H^+(aq) + HCO_3^-(aq)$	
	$HCO^-{}_3(aq) \rightleftharpoons H^+(aq) + CO_3^{2-}(aq)$	
Precipitation Reactions	$Ca^{2+}(aq) + CO_3^{2-}(aq) \rightarrow CaCO_3(s)$	Calcite
	$Fe^{2+}(aq) + CO_3^{2-}(aq) \rightarrow FeCO_3(s)$	Siderite
	$Mg^{2+}(aq) + CO_3^{2-}(aq) \rightarrow MgCO_3(s)$	Magnesite
	$Ca^{2+}(aq) + SO_4^{2-}(aq) \rightarrow CaSO_4(s)$	Anhydrite
	$K^+(aq) + 3Al^{3+}(aq) + 2SO_4^{2-}(aq) + 6H_2O(l) \rightarrow KAl_3(SO_4)_2(OH)_6(s) + 6H^+(aq)$	Alunite
	$Ca^{2+}(aq) + Mg^{2+}(aq) + 2HCO_3^-(aq) \rightarrow CaMg(CO_{3)2}(s) + 2H^+(aq)$	Dolomite

overlying an extensive aquifer with a limited support. The seismic interpretation shows that the reservoir has a gentle anticline structure with a limited number of faults crossing. The field appears to be suitable for the structural/stratigraphic trapping of CO_2 because of its dominants anticlinal structure, minor faults and the thick caprock. The fluid of the reservoir was characterized as retrograde gas, with a low range of salinity (15,000 ppm (14 g/L)). The initial pressure and temperature of the reservoir reported to be 2405 psi (16.5 MPa) and 212 °F (100 °C), respectively. The main lithology based on the core description is limestone with less than 10% dolomite, having mouldic porosity. A well, which is referred to as Well A in this study, drilled into this field in late 70s and was perforated over the interval of 4200 ft–4300 ft. The depth and lithology of different stratigraphic units are summarized in Table 3.

3. Methodology

The main objective of this study is to develop an integrated geological approach to evaluate the reservoir for its injectivity based on petrographic, core and well logs data. For this purpose, a four steps approach was followed as below:

i. Lithofacies types were identified by the petrographic analysis of core plugs obtained from Well A. The petrographic analysis was supplemented with the corroboration of the pore type and fabric against depth and temporal ranges of facies types.
ii. Lab measurements (porosity, permeability, and capillary pressure) were utilized to calibrate wireline log data which helps to understand the reservoir characteristics and lithofacies types.
iii. A composite log analysis, using gamma ray (GR), acoustic transmit-time (DT), neutron (NPHI), and density (RHOB) logs, was done to evaluate the rock properties of the reservoir. Depth corrections were made to match the core data against the corresponding wireline logs. Log based estimated properties including porosity, permeability, and water saturation were compared to the measurements made at the lab scale. An analysis was then carried out to recognize lithofacies in non-cored intervals using the log data.
iv. Having the petrographic and petrophysical interpretations, the reservoir quality of each zone was determined in terms of its porosity, permeability, thickness, water/residual gas saturation and lithofacies quality. Fig. 1 summaries the workflow of the proposed methodology described in this section.

Table 3
Interpretive geological conditions of different phases in the field.

Unit	Environment	Lithology	Formation	Depth (TOP)	Zone
Siliciclastic	Variable marine-shallow marine origin	Interbedded Sand Shale sequence	Sand and shale	820 ft	Sand horizons: 1 and 2
	Marine origin	Interbedded Sand Shale sequence	Sand and shale	1380 ft	
	Variable fluvial-marine origin	Interbedded Sand Shale sequence	Sand and shale	1650 ft	
	Marine origin	–	Shale	>1850 ft	Caprock
Transgressive cap	Offreef to open-marine	Mainly detrital packstone	Carbonate	3830 ft	1
Transitional	Offreef, reefoid and protected	Detrital foraminiferal lime packstones	Carbonate	4090 ft	2
Main build up (upper)	Protected environment	Mouldic lime packstones with two intervals of sucrosic mouldic dolomite	Carbonate	4342 ft	3
Main build up (lower)	Protected environment	Similar to previous one but homogeneous mouldic lime packstone	Carbonate	4648 ft	4

4. Analysis and interpretation

4.1. Lithological features

In this paper, lithological features were characterized by the Petrographic analysis based on the polarizing microscope (Field of view = 5 mm). All photos were taken under the crossed polarized light (XPL) except the one marked as G and H, which were taken under the plane polarized light (PPL). Thin sections were impregnated with the blue epoxy to have a better insight into the variation of porosity. DUNHAM's carbonate rock texture classification was used to recognize the depositional texture and fabrics [60]. A total number of nine lithofacies types were then recognized based on petrographic types, gross lithology (limestone/dolostone/dolomite), porosity and permeability as well as heterogeneity. In order to ascertain the occurrence of these lithofacies, modern and ancient techniques were compared. The photomicrographs of textural characteristics of these lithofacies

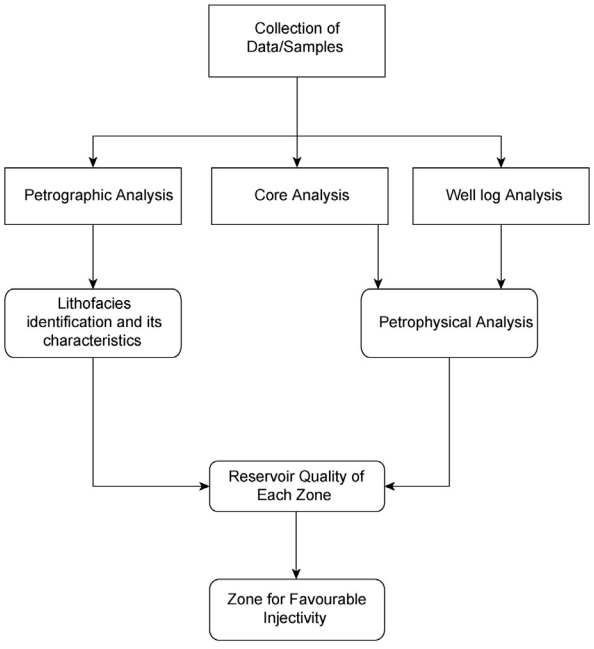

Fig. 1. The workflow of the proposed methodology used to select favourable zones for injectivity.

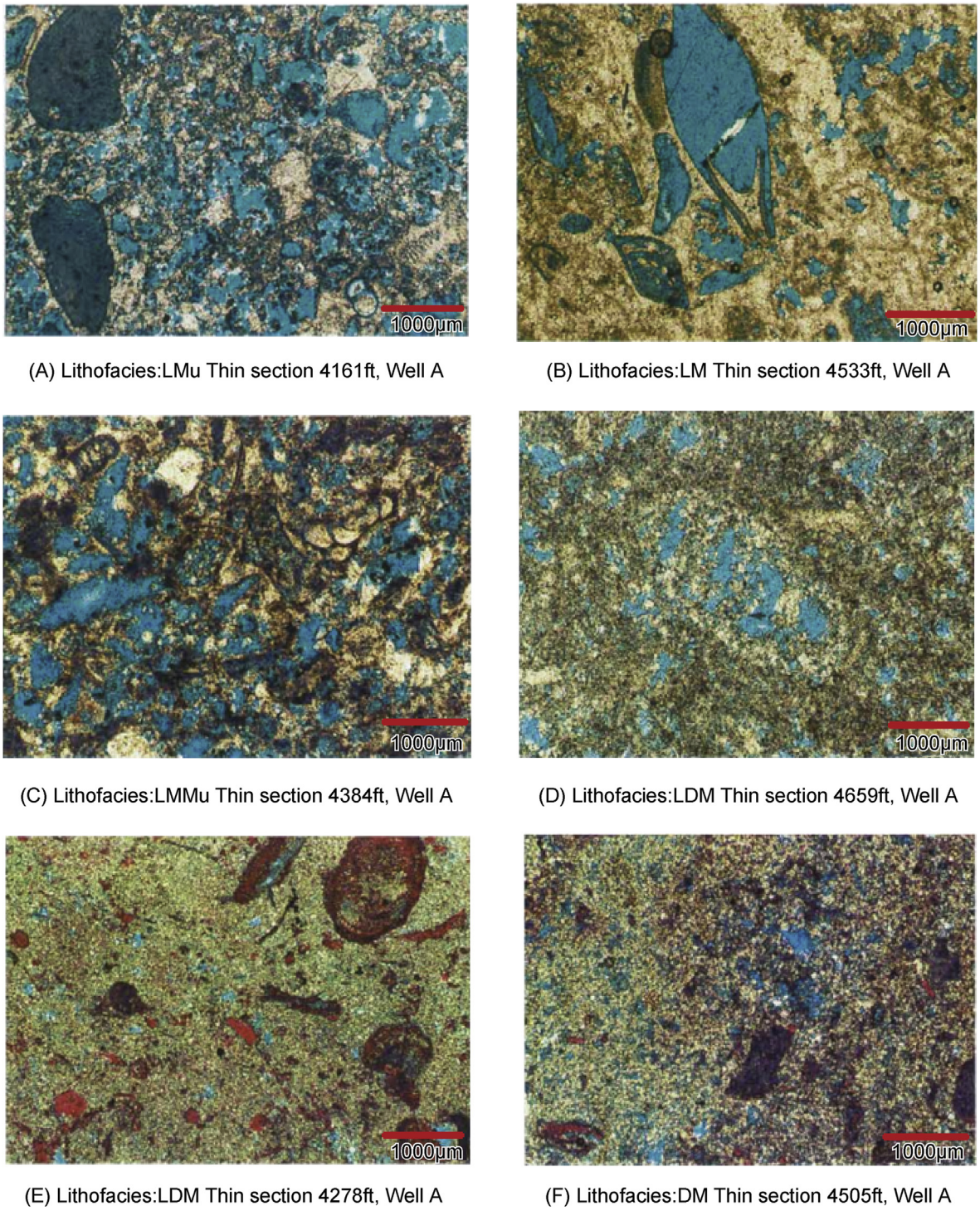

Fig. 2. Cont'd: Summary of the most common lithofacies observed in the field (Scale bar = 1 mm).

were presented in Fig. 2. Considering lithofacies classification in terms of their sediment type, porosity types, and the associated porosity and permeability measured from core samples, it was found that five out of nine lithofacies are good-quality reservoirs. They were then ranked in a descending order of the reservoir quality as: Muddy Limestone (LMu), Mouldic Limestone (LM), Muddy Mouldic Limestone (LMMu), Mouldic Dolomitic Limestone (LDM), and Mouldic Dolomite (DM). Other four lithofacies types were Tight Limestone (LT), Argillaceous Limestone (ALT), Tight Dolomitic Limestone (LDT), and Tight Dolomite (DT). These four tight and poor lithologies were denoted by the suffix of "T" in their lithofacies codes.

Generally, heterogeneity in the sediment type are beneficial to understand the characteristics of the reservoir within each lithofacies type. This is mainly because of the important role of heterogeneity in the accurate modelling of a CO_2 storage site [1]. Performing an analysis on the data of the field, it was observed that majority of lithofacies have a good total porosity which can

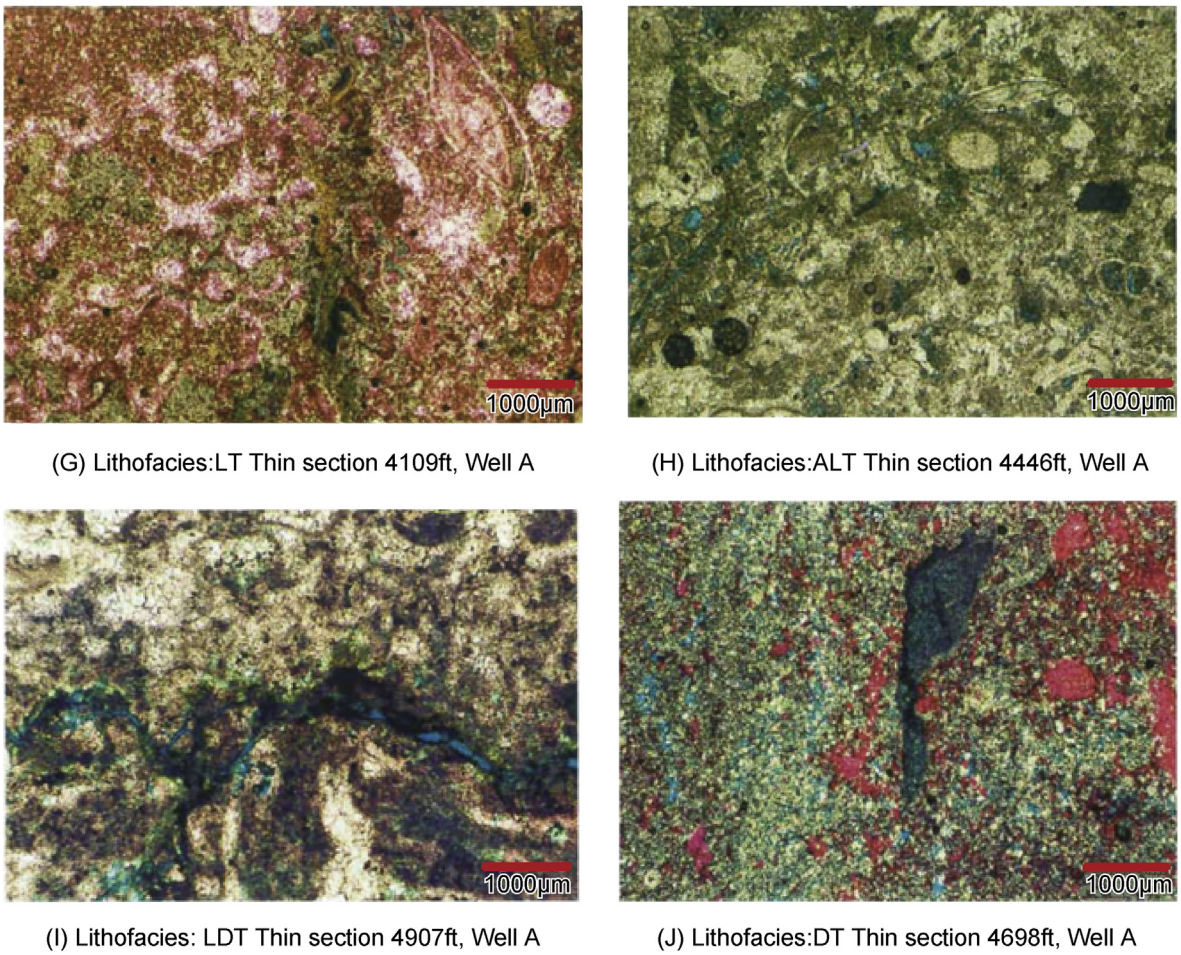

Fig. 2. (*continued*).

disperse CO_2 and entrap large fraction of the fluid phase [38]. Table 4 summarizes the features of these lithofacies in terms of their sediment type, porosity type, and porosity and permeability measured from core samples. A brief description of each lithofacies is given in the following subsections.

Considering the high dissolution [46,47] and precipitation reactions [48] rate in carbonates [29] together with fabric and rock characteristics of this carbonate field, lithofacies may precipitate as per reactions highlighted in Table 2. This precipitation may bring changes in rock characteristics with more formation

Table 4
Lithofacies descriptions of the field in terms of fabric and pore types.

ID No	Lithofacies	Depth (ft)	Well	Ø (%)	K, (mD)	Fabric	Pore types
A	Muddy Limestone (LMu)	4161	A	37.5	173	Peloidal grainstone with some bioclasts, originally, but peloids have been dissolved to form mouldic porosity (blue)	Solution-enhanced mouldic porosity
B	Mouldic Limestone (LM)	4533	A	33.5	53	Grainstone (-packstone) (blue)	Solution-enhanced mouldic porosity
C	Muddy Mouldic Limestone (LMMu)	4384	A	34.7	44	Packstone-grainstone (blue) with some bioclasts	Solution-enhanced mouldic and some Intercrystalline porosity
D	Mouldic Dolomitic Limestone (LDM)	4659	A	33.2	42	Wackestone (green), dolomitised (blue)	Mouldic and Intercrystalline porosity
E	Mouldic Dolomitic Limestone (LDM)	4278	A	20.1	23	Wackestone (green), dolomitised matrix with some bioclasts (red)	Intercrystalline porosity (bioclasts in red color are not dissolved as in A
F	Mouldic Dolomite (DM)	4505	A	26.9	16	Wackestone (green), dolomitised	mouldic and Intercrystalline porosity
G	Tight Limestone (LT)	4109	A	4.6	Nil	Grainstone-packstone (some dolomitization) Orange color-packstone	Not seen in photo-styolite associated porosity
H	Tight Argillaceous Limestone (ALT)	4446	A	5.5	3	Fine-grained argillaceous wackestone (light green)	Some Intercrystalline porosity and minor primary porosity in small forms
I	Tight Dolomitic Limestone (LDT)	4907.7	A	4.6	Nil	Grainstone-packstone with dolomitized micrite fraction (brown)	Stylolite-associated porosity (blue)
G	Tight Dolomite (DT)	4698	A	17.1	1	Mudstone-wackestone dolomitised with some bioclasts (red)	Fine Intercrystalline porosity

damage close to low-permeable areas [49], which would diminish the injectivity during the injection period [54–56].

4.1.1. Muddy Limestone (LMu)

It is the best reservoir lithofacies with a high porosity and high permeability characteristics. The sediment type is distinctive: a fine-grained, well-sorted, compacted peloidal grainstone with few bioclasts. It is characterized by solution-enhanced mouldic porosity, to the point where moulds became interconnected to develop appreciable quantities of intergranular porosity. The image analysis shows the occurrence of the narrow range of the thin-section-scale macropore sizes while the proportion of macroporosity is equal to or slightly greater than microporosity.

4.1.2. Mouldic Limestone (LM)

This lithofacies is a good quality reservoir. Heterogeneity has resulted from changes in the sediment fabric and the degree of cementation. The most common sediment type is grainstone, with pack-grainstones and some packstones. Mouldic porosity and micro-intragranular porosity are porosity types created within bioclasts and grains. Mouldic with Intercrystalline and stylolite-associated porosity are also present. This lithofacies shows the highest ratio of large pores compared to the number of micropores of all the lithofacies types. A better reservoir quality development in this lithofacies is linked to solution-enhanced pores. A series of Image analysis on the core samples shows that microporosity is dominated porosity type in this lithofacies, emphasizing the importance of microporosity to reservoir quality.

4.1.3. Muddy Mouldic Limestone (LMMu)

This lithofacies is the most common lithofacies present in the core and shows moderate to excellent reservoir characters. It is more heterogeneous than LMu and LM, in original sediment type and in the pore-type development. The petrographic type is predominantly packstones, with pack-wackestones, grainstone and boundstones. This lithofacies is characterized by a high degree of leaching which had resulted in mouldic pores (dissolved bioclasts). These pores are connected via matrix Intercrystalline or microporosity. The solution-enhanced mouldic and Intercrystalline porosity are dominated pore-types, with some mouldic and Intercrystalline porosity. More than half of the total porosity is contributed by microporosity.

4.1.4. Mouldic Dolomitic Limestone (LDM)

This lithofacies type is characterized by wackestones (green) and pack-wackestones. The heterogeneity is due to different degrees of leaching as well as primary sediment variability. Intercrystalline matrix porosity as a result of dolomitization and solution-enhanced mouldic porosity is common. Higher carbonate mud fractions occur in this lithofacies than in LMMu. Some of the pack-wackestones show cemented pores and some mouldic pores are partially reduced by the dolomite cement. The results obtained from the Image analysis shows that the contribution made to total porosity by mouldic pores in this lithofacies is far less than the DM and LM.

4.1.5. Mouldic Dolomite (DM)

There is a wide range of porosity and permeability in this poor quality lithofacies. The DM lithofacies has mouldic and Intercrystalline porosity. More than half of this porosity is contributed by microporosity. The sediment types are wackestones, and packstones. This lithofacies is characterized by Intercrystalline porosity along with mouldic porosity which was created by the dissolution of less stable bioclasts. There is a wide heterogeneity caused by differences in the proportion of bioclasts in the sediment. These characteristics indicate the porosity enhancement in the marine phreatic zone and cut-off of ambient seawater by the sediment-water interface cement.

4.1.6. Tight lithofacies (T)

Four 'tight' lithofacies description is given below:

4.1.6.1. Tight Limestone (LT). Lithofacies are predominantly tight packstones, partially cemented by calcite and associated with stylolites. The stylolites are associated with micro-intergranular porosity development.

4.1.6.2. Tight Argillaceous Limestone (ALT). The ALT is argillaceous mudstone-wackestone having a high argillaceous content which is the major cause of the reservoir quality. It can be identified by high GR readings in the tight reservoir intervals. The micritic fraction of the matrix is not substantially dolomitized. More porous streaks in the ALT are associated with the leaching around stylolites to form zones of mouldic, microintergranular to Intercrystalline porosity in streaks of packstone.

4.1.6.3. Tight Dolomitic Limestone (LDT). The LDT consists of tight wackestones, in dolomitsed fabrics Intercrystalline porosity. Other pore-types are Intercrystalline with minor mouldic porosity and stylolite-associated porosity. Mouldic pores may be occluded by the calcified anhydrite cement.

4.1.6.4. Tight Dolomite (DT). The DT is wackestone with a finely distributed porosity with some moulds in the sucrosic dolomite matrix and pore-reducing dolomite cement.

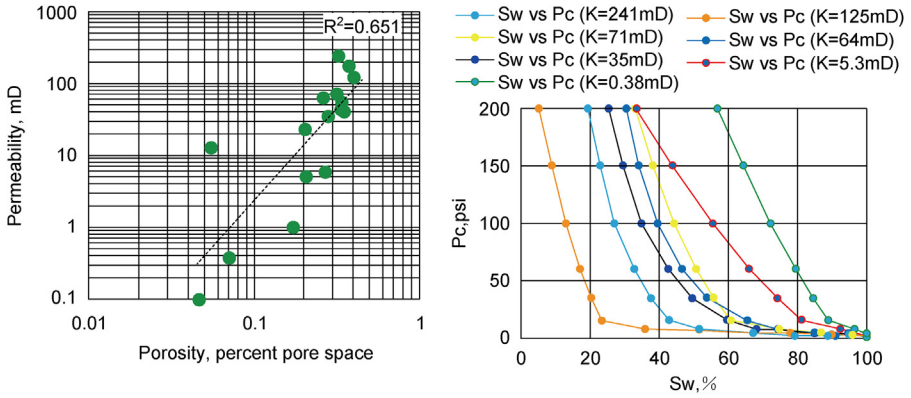

Fig. 3. Correlation between core measured porosity and permeability (left) and Capillary pressure curves of seven core plugs (right).

Table 5
Porosity, gross and net thickness of the reservoir in different wells.

Well ID	Interval of interest (ft)	Gross thickness (ft)	Net thickness (ft)	Actual perforated interval (ft)	Porosity (%)	Permeability (mD)	Residual gas/irreducible water saturation (%)
A	3942–5005	1063	847	4218–4278	26	9.13–713	31.25/9

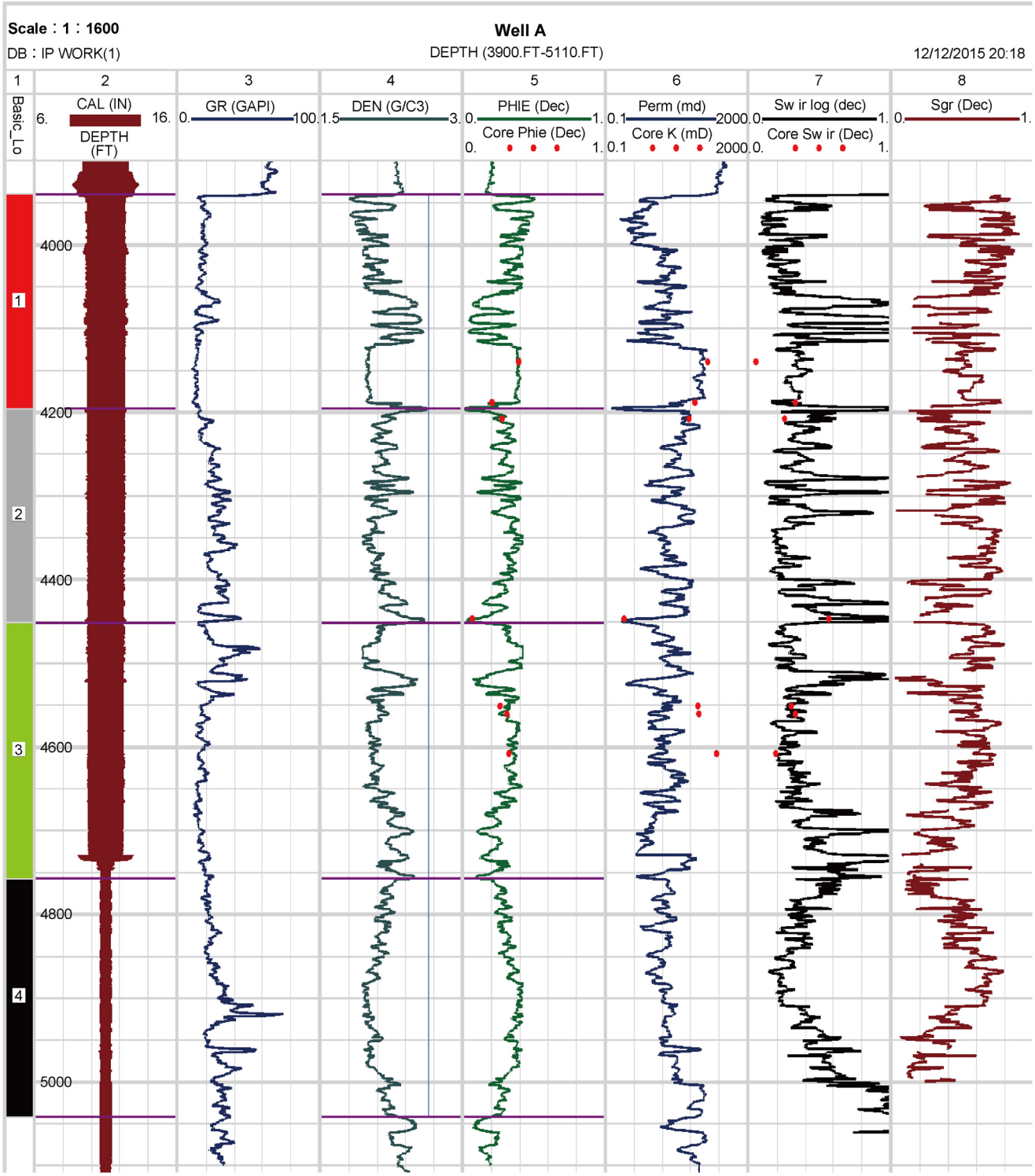

Fig. 4. Formation properties in the reservoir interval of Well A.

4.2. Petrophysical properties

Petrophysical analysis performed using wireline logs data is one of the common approaches taken to evaluate different zones in depleted oil and gas reservoirs for CO_2 storage [26,43].

For the purpose of this study, a core sample analysis for determination of petrophysical properties such as porosity, permeability and capillary pressure were done on 16 core plugs taken from different intervals of Well A. All samples were cleaned in hot refluxing methanol before being oven dried at 60 °C. This was followed by measurements of air permeability and helium porosity on the core plugs taken from 4109 ft to 4698 ft, having a wide range of porosity (4.6–39.6%) and permeability (0.38–241mD). The power regression analysis showed a reasonable correlation of 0.651 between the lab measured porosity and permeability as shown in Fig. 3.

Capillary pressure was measured on 7 core plugs by humidified air at increasing incremental pressure up to 200 psi until irreducible water saturation was reached. The degree of saturation was then determined gravimetrically after reaching the capillary equilibrium. The results of these measurements are presented in Fig. 3 (right). The Leverett up-scaling relationship was used to characterize capillary heterogeneity and generate a single reservoir curve, where the relative permeability was assumed uniform [61]. Attempts were made to average the capillary pressure curves using J-function but it was not successful. It might be due to the effect of heterogeneity and the complex diagenetic phenomenon caused by the presence of many lithofacies types [62].

There are a total of five zones separated by tight layers. Well A is intersecting four of these zones except the flank zone which is on both sides of the reservoir. The well log data was used in the next step to evaluate the porosity, net thickness, permeability and the residual gas/water saturation as given in Table 5. Fig. 4 shows the interpreted logs of this study. The first track in this Figure is the interval where the reservoir has been divided into four main zones based on the density log. The second track shows the depth and calliper log (Cal). The third to sixth tracks include the gamma ray log, bulk density, porosity, permeability, and irreducible water saturation logs. The residual gas saturation shown in the last track of this figure was estimated by the approach developed by Ransom and Holm [63] is given in the last track.

For the interpretation purpose, the porosity cut-off was obtained as 10%, and the favourable thickness (net pay) was estimated as 847.75 ft (258 m). Based on the wellbore condition as well as GR, density, porosity, and permeability responses, the favourable interval for the injection was indicated to be 3942–5005 ft (1201–1525.5 m). The results obtained also revealed that the effective porosity estimated using the wireline logs has a good match with the lab measured porosity with a correlation of 0.91 (see Fig. 5). The estimated permeability using the Timur's correlation, however, showed a weak match with the lab measured permeability based on the correlation of 0.44 (see Fig. 5). It was also found that permeability decreases with depth, from a maximum value of 713 mD at 4141 ft to 9.13 mD at 4698 ft. Porosity and permeability estimated from the logs considering the initial water saturation (Sw_i) were then correlated and gave a good correlation of 0.82 as shown in Fig. 6. It is generally known that recognitions of lithofacies from wireline logs in the non-cored intervals of the well is essential to have an accurate modelling of the storage site. However, due to lateral heterogeneity observed in the analysis, the lithofacies obtained could not be extended for the non-cored intervals using the well log response. Table 6 gives the rock/fluid characteristics of different zones observed through the wireline log data.

There are several constraints which may affect the injection operation if the chosen reservoir has a remarkable water or gas saturations. As a result, the irreducible water saturation was estimated using porosity and resistivity logs and compared with that of the capillary pressure test data. It was then found that this saturation is quite different in various zones and it has a

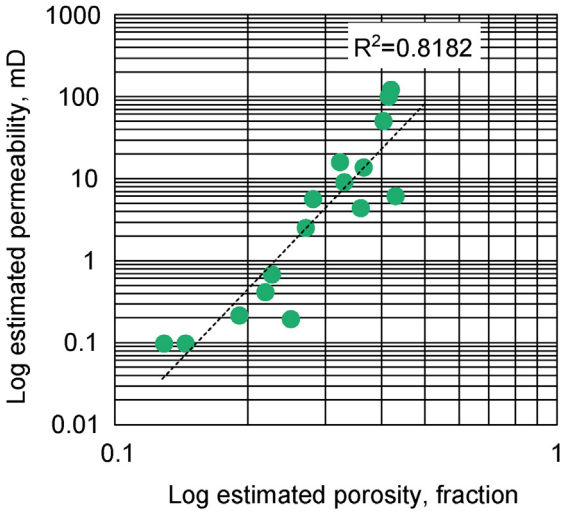

Fig. 6. Correlation between log estimated porosity and permeability.

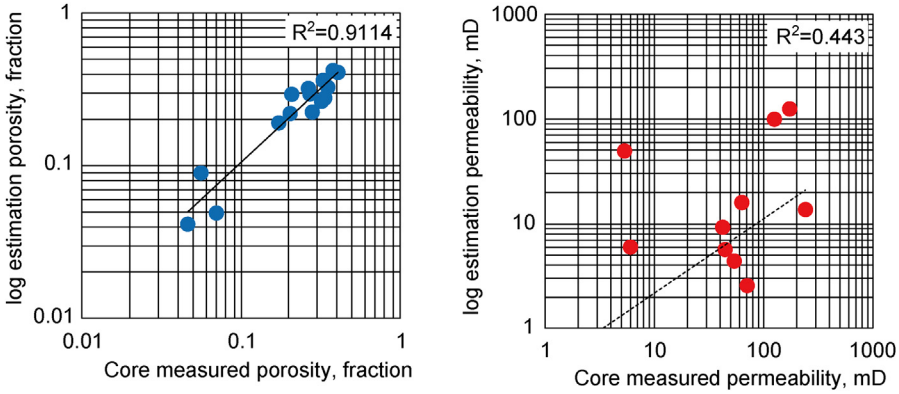

Fig. 5. Correlation between laboratory and log measured porosity (left); correlation between laboratory and log measured permeability (right).

Table 6
Rock/fluid characteristics of different zones obtained from wireline log data.

Parameters	Zone1	Zone2	Zone3	Zone4
Depth, ft	3942 −4200	4200 −4470	4470 −4720	4720 −5005
Porosity, %	25.3	26.2	27.5	24.5
Thickness (net) ft	258	270	250	285
Permeability (near-wellbore) mD	81	161.75	172	121.44
Average residual gas/water saturation, %	36/7	30/9	26/6	33/13

maximum value in tight formations of the field. This high percentage of water saturation can significantly reduce the chance of having an effective storage capacity [36,37]. Residual gas saturation which may also affect the efficiency of injectivity [18,34] can be estimated using deep and shallow resistivity logs and the approach presented by Ransom and Holm [63], which is applicable to both oil and gas reservoirs. The results obtained revealed that the residual gas saturation is ranging from 36% to 66% within the reservoir and its average value (31.25%) is near to the thermal decay time log (TDT) measurements (30% S_{gr}). The average residual gas saturation within the interval of zone No. 2 and zone No. 3 is less than that of the zone No. 1 and zone No. 4.

As mentioned earlier, the amount of the remaining oil in retrograde gas media may also affect the CO_2 relative permeability and, hence, CO_2 injectivity [35]. According to the field report, proven and expected ultimate recovery of condensate could be 18 MMSTB (million stock tank barrel) and 28MMSTB, respectively. At the recovery factor of 60%, the remaining condensate could influence injectivity and, therefore, more recovery of condensate via the enhanced recovery process would be useful to have a favourable CO_2 injectivity [35].

It can safely say that the interpretation provided based on the wireline log data combined with the results of the core analysis could be useful to highlight the potential zones. Based on the above petrophysics analysis, it can be concluded that the level of heterogeneity as depicted by the capillary pressure and lithofacies analysis could play a crucial role in controlling brine displacement upon CO_2 injection which has a major influence on the plume migration and storage capacity [38,39]. Having a reasonable match of log estimated porosity, permeability and water saturation with the measured core data, field zones at a suitable depth and pressure-temperature conditions with different rock/fluid characteristics will be selected for having a successful injection operation. Hence, it would be wised to experimentally or numerically evaluate injectivity by considering the residual constraints (fraction of water, remaining gas and condensate (oil phase)) as it varies with the injection rates, salinity of formation water [50], and carbonate mineralization [51].

5. Reservoir quality and CO_2 injectivity

Petrophysical evaluations of the reservoir alone suggested that it could provide a reasonable injectivity due to its high porosity and permeability, together with high quality facies [64–66]. In this study, the lithofacies analysis indicates that porosity developments are related to the original sediment type and smaller-scale depositional cyclicity. Late-leaching had made a significant positive contribution into the reservoir quality, especially in packstone and grainstone lithofacies. A relationship was found between the lithofacies and original sediment type including peloidal grainstone, packstones, wackestone, and pack-wackestones. The heterogeneities in the sediment type are useful to understand the characteristics of the reservoir within each lithofacies type. The secondary diagenetic pore types developed in these lithofacies are controlled by the primary sediment fabric.

The texture of dolomitized lithofacies was recognized purely fabric-selective to the micritic carbonate mud fraction. Therefore, dolomitic lithofacies (LDM and DM) are predominantly wackestones or pack-wackestones. The muddy matrix in packstones has undergone dolomitization and caused the development of Intercrystalline porosity by the dissolution of bioclasts. Packstones have a higher proportion of grains in the matrix than wackestones, and, thus, the mouldic Intercrystalline or microporosity porosity dominant. Each lithofacies with microporosity accounts for approximately half of the total porosity of the reservoir lithofacies when it is compared with the visible mouldic pores.

The solution-enhancement is common in packstone lithofacies (LMMu) and shows an excellent reservoir character. In grainstone, composed of LM facie, original porosity has been cemented with calcite, and mouldic and/or intergranular/micro intergranular porosity developed in bioclasts and peloids. The reservoir quality in this lithofacies has been reduced by mouldic porosity which is very well connected. However, late-leaching along with open stylolites is one of the major characteristics of this lithofacies which improves the reservoir quality. LDT lithofacies has a low Stylolite-associated porosity and permeability [67].

Lithofacies such as LMu, LM and LMMu have a solution enhanced mouldic porosity and permeability while DM is a low reservoir quality facies. The lithofacies 'T' are characterized by a low porosity and permeability, creating a poor reservoir quality. Moreover, different levels of porosity and permeability observed through the well log data interpretation together with failure to average the capillary pressure data revealed that there is a wide variation of the facies obtained as mentioned and obtained earlier by the petrographic analysis. It is, therefore, concluded that there are four zones with different levels of reservoir quality with lateral heterogeneity.

For a favourable injectivity, the reservoir at the depth of greater than 2625 ft seems to have a good permeability, porosity, and thickness with a low level of water/gas saturation for achieving a maximum storage capacity. The analysis of a wide range of data obtained from well A indicates that the zone No. 2 and 3 are good quality zones with a favourable thickness which can support a high injection rate. According to Chadwick et al. [44] and Raza et al. [45], the thickness should be greater than 164 ft for a successful CO_2 injection. Overall, the zone No. 3 due to having a good thickness (250 ft), good-quality facies with a favourable porosity and permeability and a small amount of residual gas/water saturation shows a better reservoir quality compared to the zone No. 2. The zone No. 1, on the other hand, should not be selected at all for the injection practice. The zone No. 4 is a very low quality interval connected to a wide spread aquifer which should not be chosen as a part of the storage practice. Thus, the intervals from 4200 ft to 4470 ft (i.e., zone 2) and 4470 ft to 4720 ft (i.e., zone 3) are the best intervals for the injection. Table 7 depicts the characteristics of different zones considered as part of the favourable target selection for a safe storage practice.

It is indicated that tight zones can act as barriers to slow down the vertical flow of CO_2 [40,68]. According to Frykman et al. [68], numerical modelling of the Vedsted structure composed of two different facies in Denmark revealed that layers of poor quality facies with intraformational sealing can slow down the vertical flow of CO_2. Having said that, it seems that having those tight layers (low permeable) in the field can help to achieve a good storage capacity due to the slow vertical movement of CO_2.

Table 7
Comparing characteristics of different zones for an optimum injectivity target selection.

Parameters	Positive indicator	Negative indicator	Zone1	Zone2	Zone3	Zone4
Depth, ft	>2625 ft (800 m)	2625 ft (800 m) > depth > 6562 ft (2000 m)	3942–4200	4200–4470	4470–4720	4720–5005
CO_2 density	high	low	Field pressure and temperature conditions			
Porosity, %	>20%	<10%	25.3	26.2	27.5	24.5
Thickness, ft	≫164 ft(50 m)	<66 ft(20 m)	258	270	250	285
Permeability (near-wellbore), mD	>100mD	10–100 mD	81	161.75	172	121.44
Pore throat size distribution	Less heterogeneous	Highly heterogeneous	High Variation of rock fabrics in 4109 ft–4698 ft interval			
Average residual gas/water saturation, %	low	high	36/7	30/9	26/6	33/13
Condensate (oil phase) saturation	low	high	Expected 40% Condensate (oil phase) at depleted stage			
Lithofacies types	Good Quality	Low Quality	LMu, LT	LMMu, LDM, ALT	LM, LDM,DM,DT	LDT

However, it worth to evaluate the injectivity through numerical and experimental studies on the zones suggested by this study to ensure that the interval can support a high injection rate. Additionally, an evaluation on CO_2/brine/rock chemical reactions, and the influence of both brine chemistry and CO_2 composition before selecting any carbonate formations as a storage site would also be useful to make a final decision.

6. Conclusions

In this paper, quality of a reservoir located in Malaysia was evaluated to provide a better insight into its suitability for a CO_2 storage practice. An injectivity analysis was done based on the facies and petrophysical descriptions considering different indicators for target selections. The reservoir was found to be highly heterogeneous, undergone through a complex diagenetic phenomenon which controls the brine displacement upon CO_2 injection as well as plume migration and storage capacity. Based on the facies characterization, the reservoir has classified into nine lithofacies where lithofacies marked by A-E show a good quality. Four zones separated by tight layers were marked based on the wireline log interpretation at different intervals, having different rock/fluid characteristics. The integrated analysis indicated that the zone No. 2 and 3 are rational choices for injection because of their favourable characteristics.

The methodology presented in this study can be useful for evaluation of injectivity in the depleted storage sites during CO_2 storage site selection. This study will be continued to further evaluate the injectivity of each zone through numerical and experimental analysis by considering other constraints such as fraction of water, remaining gas and condensate, and CO_2/brine/rock chemical reactions.

Acknowledgment

The authors would like to acknowledge “Curtin University Sarawak Malaysia” for funding this research through the Curtin Sarawak Research Institute (CSRI) Flagship scheme under the grant number CSRI 6015. We would like to thank Senergy Limited for the license of Interactive Petrophysics tool.

References

[1] J. Ennis-King, T. Dance, J. Xu, C. Boreham, B. Freifeld, C. Jenkins, L. Paterson, S. Sharma, L. Stalker, J. Underschultz, The role of heterogeneity in CO_2 storage in a depleted gas field: history matching of simulation models to field data for the CO2CRC Otway Project, Australia, Energy Procedia 4 (2011) 3494–3501.

[2] S. Solomon, Carbon dioxide storage: geological security and environmental issues–case study on the Sleipner Gas field in Norway, Bellona Rep. (2007) 7–120.

[3] I.W. Wright, The in salah gas CO_2 storage project, in: IPTC 2007: International Petroleum Technology Conference, 2007.

[4] W. Zhou, M.J. Stenhouse, R. Arthur, S. Whittaker, D.H.S. Law, R. Chalaturnyk, W. Jazrawi, The IEA Weyburn CO2 monitoring and storage project — modeling of the long-term migration of CO2 from Weyburn, in: E.S.R.W.K.F.G. Wilson, T.M.G. Thambimuthu (Eds.), Greenhouse Gas Control Technologies 7, Elsevier Science Ltd, Oxford, 2005, pp. 721–729.

[5] T.J. Tambach, M. Koenen, L.J. Wasch, F. van Bergen, Geochemical evaluation of CO_2 injection and containment in a depleted gas field, Int. J. Greenh. Gas Control 32 (0) (2015) 61–80.

[6] M.A. Barrufet, A. Bacquet, G. Falcone, Analysis of the Storage Capacity for CO_2 Sequestration of a Depleted Gas Condensate Reservoir and a Saline Aquifer, Society of Petroleum Engineers, 2010. SPE-139771-PA.

[7] J. Narinesingh, D. Alexander, CO_2 Enhanced gas recovery and geologic sequestration in condensate reservoir: a simulation study of the effects of injection pressure on condensate recovery from reservoir and CO_2 storage efficiency, Energy Procedia 63 (2014) 3107–3115.

[8] L. Sobers, S. Frailey, A. Lawal, Geological sequestration of carbon dioxide in depleted gas reservoirs, in: SPE/DOE Symposium on Improved Oil Recovery, Society of Petroleum Engineers, 2004.

[9] A.S. Al-Abri, Enhanced Gas Condensate Recovery by CO_2 Injection, Doctoral dissertation, Curtin University of Technology, Faculty of Science and Engineering, Department of Petroleum Engineering, 2011.

[10] C.H. Shen, B.Z. Hsieh, C.C. Tseng, T.L. Chen, Case study of CO_2-IGR and storage in a nearly depleted gas-condensate reservoir in Taiwan, Energy Procedia 63 (2014) 7740–7749.

[11] C. Yuan, Z. Zhang, K. Liu, Assessment of the recovery and front contrast of CO_2 EOR and sequestration in a new gas condensate reservoir by compositional simulation and seismic modeling, Fuel 142 (2015) 81–86.

[12] K. Bedard, M. Malo, Y. Duchaine, E. Konstantivovskaya, B. Giroux, Potential CO_2 Geological Storage Sites for Carbon Capture and Storage (CCS) in Québec St. Lawrence Lowlands-a Preliminary Analysis, 2010, pp. 1–4. AAPG Search and Discovery Article #90172 © CSPG/CSEG/CWLS GeoConvention 2010, Calgary, Alberta, Canada.

[13] Z. Fang, X. Li, Preliminary assessment of CO_2 geological storage potential in Chongqing, China, Procedia Environ. Sci. 11 (Part C) (2011) 1064–1071.

[14] A. Ramírez, S. Hagedoorn, L. Kramers, T. Wildenborg, C. Hendriks, Screening CO_2 storage options in The Netherlands, Int. J. Greenh. Gas Control 4 (2) (2010) 367–380.

[15] M.A. Barrufet, A. Bacquet, G. Falcone, Analysis of the storage capacity for CO_2 sequestration of a depleted gas condensate reservoir and a saline aquifer, J. Can. Pet. Technol. 49 (08) (2010) 23–31.

[16] M. Jalil, M.R. Masoudi, N.B. Darman, M. Othman, Study of the CO_2 injection storage and sequestration in depleted M4 carbonate gas condensate reservoir Malaysia, in: Carbon Management Technology Conference, 2010, pp. 1–8. Carbon Management Technology Conference.

[17] C. Belgodere, J. Sterpenich, J. Pironon, A. Randi, J.P. Birat, Experimental study of CO_2 injection in the triassic sandstones of lorraine (eastern France)–Investigation of injection well injectivity impairment by mineral precipitations, in: Le Studium Conference. Geochemical Reactivity in CO_2, 2014, pp. 1–5.

[18] A. Saeedi, R. Rezaee, Effect of residual natural gas saturation on multiphase flow behaviour during CO_2 geo-sequestration in depleted natural gas reservoirs, J. Pet. Sci. Eng. 82–83 (0) (2012) 17–26.

[19] A. Saeedi, Experimental Study of Multiphase Flow in Porous Media During CO_2 Geo-Sequestration Processes, Springer Science & Business Media, 2012, pp. 1–100.

[20] Y. Peysson, L. Andre, M. Azaroual, Well injectivity during CO_2 storage operations in deep saline aquifers{Part 1: experimental investigation of drying effects, salt precipitation and capillary forces, Int. J. Greenh. Gas Control 22 (2013) 291–300.

[21] H. Geistlinger, S. Mohammadian, Capillary trapping mechanism in strongly water wet systems: comparison between experiment and percolation theory, Adv. Water Resource 79 (0) (2015) 35–50.
[22] J. Lu, M. Kordi, S.D. Hovorka, T.A. Meckel, C.A. Christopher, Reservoir characterization and complications for trapping mechanisms at Cranfield CO_2 Injection Site, Int. J. Greenh. Gas Control 18 (0) (2013) 361–374.
[23] S.A. Shedid, A.M. Salem, Experimental investigations of CO2 solubility and variations in petrophysical properties due to CO2 storage in carbonate reservoir rocks, in: North Africa Technical Conference and Exhibition, Society of Petroleum Engineers, 2013, pp. 1–9.
[24] Y. Zhang, L. Langhi, P.M. Schaubs, C.D. Piane, D.N. Dewhurst, L. Stalker, K. Michael, Geomechanical stability of CO_2 containment at the South West Hub Western Australia: a coupled geomechanical–fluid flow modelling approach, Int. J. Greenh. Gas Control 37 (2015) 12–23.
[25] T. Ito, T. Nakajima, S. Chiyonobu, Z. Xue, Petrophysical properties and their relation to injected CO_2 behavior in a reservoir at the Nagaoka pilot site, Japan, Energy Procedia 63 (0) (2014) 2855–2860.
[26] H.K.H. Olierook, C. Delle Piane, N.E. Timms, L. Esteban, R. Rezaee, A.J. Mory, L. Hancock, Facies-based rock properties characterization for CO_2 sequestration: GSWA Harvey 1 well, Western Australia, Mar. Pet. Geol. 50 (2014) 83–102.
[27] S. Bachu, Screening and ranking of sedimentary basins for sequestration of CO_2 in geological media in response to climate change, Environ. Geol. 44 (3) (2003) 277–289.
[28] D. Qi, S. Zhang, K. Su, Risk assessment of CO_2 geological storage and the calculation of storage capacity, Pet. Sci. Technol. 28 (10) (2010) 979–986.
[29] A. Raza, R. Rezaee, R. Gholami, V. Rasouli, C.H. Bing, R. Nagarajan, M.A. Hamid, Injectivity and quantification of capillary trapping for CO_2 storage: a review of influencing parameters, J. Nat. Gas Sci. Eng. 26 (2015) 510–517.
[30] W. Han, K. Kim, R. Esser, E. Park, B. McPherson, Sensitivity study of simulation parameters controlling CO_2 trapping mechanisms in saline formations, Transp. Porous Media 90 (3) (2011) 807–829.
[31] H. Shamshiri, B. Jafarpour, Controlled CO_2 injection into heterogeneous geologic formations for improved solubility and residual trapping, Water Resource Res. 48 (2) (2012).
[32] Y. Cinar, O. Bukhteeva, P.R. Neal, W.G. Allinson, L. Paterson, CO2 Storage in low permeability formations, in: SPE Symposium on Improved Oil Recovery, Society of Petroleum Engineers, 2008.
[33] S.M. Ghaderi, D.W. Keith, Y. Leonenko, Feasibility of injecting large volumes of CO_2 into aquifers, Energy Procedia 1 (1) (2009) 3113–3120.
[34] C. Oldenburg, C. Doughty, Injection, flow, and mixing of CO_2 in porous media with residual gas, Transp. porous media 90 (1) (2011) 201–218.
[35] A.R. Kovscek, Screening criteria for CO_2 storage in oil reservoirs, Pet. Sci. Technol. 20 (7–8) (2002) 841–866.
[36] C.H. Pentland, R. El-Maghraby, A. Georgiadis, S. Iglauer, M.J. Blunt, Immiscible displacements and capillary trapping in CO_2 storage, Energy Procedia 4 (0) (2011) 4969–4976.
[37] T. Suekane, T. Nobuso, S. Hirai, M. Kiyota, Geological storage of carbon dioxide by residual gas and solubility trapping, Int. J. Greenh. Gas Control 2 (1) (2008) 58–64.
[38] A. Honari, B. Bijeljic, M.L. Johns, E.F. May, Enhanced gas recovery with CO_2 sequestration: the effect of medium heterogeneity on the dispersion of supercritical CO_2–CH_4, Int. J. Greenh. Gas Control 39 (2015) 39–50.
[39] H. Ott, C.H. Pentland, S. Oedai, CO_2–brine displacement in heterogeneous carbonates, Int. J. Greenh. Gas Control 33 (2015) 135–144.
[40] C. Ukaegbu, O. Gundogan, E. Mackay, G. Pickup, A. Todd, F. Gozalpour, Simulation of CO_2 storage in a heterogeneous aquifer, Proc. Inst. Mech. Eng. 223 (2009) 249–267.
[41] P. Frykman, C.M. Nielsen, N. Bech, Trapping effects of small scale sedimentary heterogeneities, Energy Procedia 37 (0) (2013) 5352–5359.
[42] D. Ito, T. Matsuura, M. kamon, K. Kawada, M. Nishimura, S. Tomita, A. katoh, A.K. Akaku, T. Inamori, Y. Yamanouchi, J. Mikami, Reservoir evaluation for the moebetsu formation at tomakomai candidate site for ccs demonstration project in Japan, Energy Procedia 37 (0) (2013) 4937–4945.
[43] O. Akintunde, C. Knapp, J. Knapp, Petrophysical characterization of the south Georgia rift basin for supercritical CO_2 storage: a preliminary assessment, Environ. Earth Sci. 70 (7) (2013) 2971–2985.
[44] A. Chadwick, R. Arts, C. Bernstone, F. May, S. Thibeau, P. Zweigel, Best practice for the storage of CO_2 in saline aquifers, Br. Geol. Surv. Occas. Publ. 14 (2008) 267.
[45] A. Raza, R. Rezaee, R. Gholami, C.H. Bing, R. Nagarajan, M.A. Hamid, A screening criterion for selection of suitable CO_2 storage sites, J. Nat. Gas Sci. Eng. 28 (2016) 317–327.
[46] D.N. Espinoza, S.H. Kim, j.C. Santamarina, CO_2 geological storage—geotechnical implications, KSCE J. Civ. Eng. 15 (4) (2011) 707–719.
[47] S.M. Farquhar, J.K. Pearce, G.K.W. Dawson, A. Golab, S. Sommacal, D. Kirste, D. Biddle, S.D. Golding, A fresh approach to investigating CO_2 storage: experimental CO_2–water–rock interactions in a low-salinity reservoir system, Chem. Geol. 399 (2015) 98–122.
[48] G.P.D. De Silva, P.G. Ranjith, M.S.A. Perera, Geochemical aspects of CO_2 sequestration in deep saline aquifers: a review, Fuel 155 (2015) 128–143.
[49] I. Mohamed, H.A. Nasr-El-Din, Fluid/rock interactions during CO_2 sequestration in deep saline carbonate aquifers: laboratory and modeling studies, SPE J. 18 (03) (2013) 468–485.
[50] O. Izgec, B. Demiral, H. Bertin, S. Akin, CO_2 injection into saline carbonate aquifer formations I: laboratory investigation, Transp. Porous Media 72 (1) (2008) 1–24.
[51] S. Yoo, T. Myojo, T. Matsuoka, A. Ueda, Experimental studies of injectivity reduction due to carbonate mineralization, Procedia Earth Planet. Sci. 7 (0) (2013) 920–923.
[52] H. Alkan, Y. Cinar, E.B. Ülker, Impact of capillary pressure, salinity and in situ conditions on CO_2 injection into saline aquifers, Transp. Porous Media 84 (3) (2010) 799–819.
[53] T. Giorgis, M. Carpita, A. Battistelli, 2D Modeling of salt precipitation during the injection of dry CO_2 in a depleted gas reservoir, Energy Conv. Manag. 48 (6) (2007) 1816–1826.
[54] L. Andre, Y. Peysson, M. Azaroual, Well injectivity during CO_2 storage operations in deep saline aquifers – Part 2: numerical simulations of drying, salt deposit mechanisms and role of capillary forces, Int. J. Greenh. Gas Control 22 (0) (2014) 301–312.
[55] H. Ott, S.M. Roels, K. de Kloe, Salt precipitation due to supercritical gas injection: I. Capillary-driven flow in unimodal sandstone, Int. J. Greenh. Gas Control (0) (2015) 1–9.
[56] S. Yoo, T. Myojo, T. Matsuoka, A. Ueda, Experimental studies of injectivity reduction due to carbonate mineralization, Procedia Earth Planet. Sci. 7 (0) (2013) 920–923.
[57] N. Kampman, M. Bickle, M. Wigley, B. Dubacq, Fluid flow and CO_2–fluid–mineral interactions during CO_2-storage in sedimentary basins, Chem. Geol. 369 (0) (2014) 22–50.
[58] A. Raza, R. Gholami, M. Sarmadivaleh, N. Tarom, R. Rezaee, C.H. Bing, R. Nagarajan, M.A. Hamid, H. Elochukwu, Integrity analysis of CO_2 storage sites concerning geochemical-geomechanical interactions in saline aquifers, J. Nat. Gas Sci. Eng. 36PA (2016) 224–240.
[59] T. Kovacs, D.F. Poulussen, C.d. DiosvCIUDEN, Strategies for Injection of CO2 into Carbonate Rocks, Global Carbon Capture and Storage Institute Ltd, 2015.
[60] R.J. Dunham, Classification of carbonate rocks according to depositional texture, in: W.E. Ham (Ed.), Classification of Carbonate Rocks, AAPG, Tulsa, 1962, pp. 108–121.
[61] C.W. Kuo, S.M. Benson, Numerical and analytical study of effects of small scale heterogeneity on CO_2/brine multiphase flow system in horizontal corefloods, Adv. Water Resource 79 (0) (2015) 1–17.
[62] B. Ataie-Ashtiani, S. Majid Hassanizadeh, M.A. Celia, Effects of heterogeneities on capillary pressure–saturation–relative permeability relationships, J. Contam. Hydrol. 56 (3) (2002) 175–192.
[63] R.C. Ransom, and L.R.W. Holm, Determining Residual Oil Saturation Following Flooding. U.S. Patent No. 4,102,396. Washington, DC: U.S. Patent and Trademark Office (1978) 1–7.
[64] G. Atkinson, S. Bloch, M. Scheihing, Sedimentology and depositional environments of the oligo-miocene gas-bearing succession in the yacheng 13–1 field, south China sea, People's Republic of China, AAPG Bull. 74 (1990) 601.
[65] S. Bloch, Empirical prediction of porosity and permeability in sandstones (1), AAPG Bull. 75 (7) (1991) 1145–1160.
[66] J. McGowen, S. Bloch, Depositional facies, diagenesis, and reservoir quality of ivishak sandstone (Sadlerochit Group), Prudhoe Bay Field: ABSTRACT, AAPG Bull. 69 (2) (1985), 286–286.
[67] A.S. Alsharhan, Stylolites in Lower Cretaceous Carbonate Reservoirs, Society for sedimentary geology, UAE, 2000, pp. 1–3.
[68] P. Frykman, N. Bech, A.T. Sørensen, L.H. Nielsen, C.M. Nielsen, L. Kristensen, T. Bidstrup, Geological modeling and dynamic flow analysis as initial site investigation for large-scale CO_2 injection at the Vedsted structure, NW Denmark, Energy Procedia 1 (1) (2009) 2975–2982.